JOURNAL OF COMPUTATIONAL PHYSICS 9, 424–439 (1972)

Initial Value Techniques in Free-Surface Hydrodynamics

C. R. EASTON

Propulsion Department, Research and Development Subdivision, McDonnell Douglas Astronautics Company-West, Huntington Beach, California 92647

AND

IVAN CATTON

School of Engineering and Applied Science, University of California, Los Angeles, California 90024

Received January 21, 1971

A general technique for solving the nonlinear, transient motion of a liquid with a free surface has been developed. The liquid is assumed to be irrotational and incompressible. The solution technique combines an analytical solution to the continuity equation with numerical solutions of the equations governing the location and velocity potential of the free surface. The numerical integration of the free surface boundary conditions is a very sensitive step in the solution. Because of the extreme importance of this step, a survey of integration techniques was made. Six frequently proposed methods for performing the integration were screened by calculating a nonlinear, free oscillation and monitoring total system energy. All methods were numerically consistent but the Euler-backward, leapfrog trapezoidal, and Heun methods were the only methods which were even conditionally stable. This result is in contrast with previous studies of linear equations, for which all of the surveyed methods were stable.

1. INTRODUCTION

Large amplitude motions of liquids with free surfaces occur in problems ranging from space technology to oceanology and even underground hydrology. In many of these problems, such as propellant resettling and breaking waves, viscous effects and rotationality are important. It is necessary to use a general computational technique such as the marker-and-cell Method (MAC) [1], to calculate solutions to problems such as these.

There are many other problems which may be successfully treated by analytical or analytical/numerical techniques by assuming incompressible, irrotational flow. Among these are draining of liquid from a container [2], unsettling of a propellant [3], sloshing [4], movement of large gravity waves [5], and capillary waves [6]. The techniques used for solving these problems share the common advantage of

being computationally much more efficient than the more general methods such as MAC. For example, the liquid draining solution of [2] required less than 1/10th the computation time required for solution by MAC. These techniques also share the potential of being free, or nearly free of diffusive truncation errors, a common malady of finite difference techniques (Daly [7], and Hirt [8]). Of the analytical/numerical techniques referenced above, those of Easton and Catton [2], and Moore and Perko [3], are suitable for the solution of initial value problems such as draining, unsettling and aperiodic sloshing. These two techniques are similar in that they both employ numerical solution of the free surface boundary conditions. The methods differ in that Easton and Catton use the Galerkin method to meet the free surface boundary conditions. Moore and Perko use orthonormalization to define a set of functions which are orthonormal to the series evaluated on the free surface. When the nonlinear surface tension term is included, no such set of functions can be calculated. Therefore, Moore and Perko were forced to use an approximate treatment of surface tension which only works when surface tension is not important [9]. In addition to being able to correctly treat surface tension, the Easton and Catton technique is very rapid in execution and apparently uses much less computer storage [10], a very significant advantage with the modern multiprocessor computer.

Of the computational methods surveyed, only the fully numerical solutions and the Easton and Catton solution were able to include nonlinear effects, surface tension, and gravitation. However, subsequent attempts to calculate other flows by the method of [2] revealed that the initial value technique employed for the solution of the surface equations was inadequate. The difficulty was traced to a truncation error arising from the finite difference representation of derivatives with respect to time.

There are several explicit techniques for integrating the free surface boundary condition equations. Kurihara studied the stability and accuracy of solution techniques for the linear one-dimensional wave equation. Stability and accuracy of time-differencing schemes were also studied by Lilly [12] for the vorticity transport equation, using spectral analysis for the spatial derivatives. The analyses presented in these papers have shown that the differencing techniques can either damp or amplify disturbances in the flow. These inaccuracies are particularly important in the solution of the nonlinear equations governing potential flow of a liquid with a free surface. Therefore, the accuracy and stability of the various solution techniques was studied for the problem of a symmetric, free oscillation.

Conservation of total system energy was used as the measure of accuracy .The general technique used for solving the potential flow problem was described by Easton and Catton [2], and Easton [13]. This method is summarized in Section 2. The initial value techniques employed are described in Section 3 and results are presented in Section 4.

2. Solution Technique for Potential Flow

Equations and Boundary Conditions

The equations governing incompressible, irrotational (inviscid) flow are well known. Any of the basic texts, such as Lamb [14], may be used for reference.

The equation of continuity, or conservation of mass, for an incompressible, irrotational fluid may be expressed in terms of velocity potential by

$$\nabla^2\phi = 0. \tag{1}$$

For convenience, ϕ is made dimensionless, such that

$$\mathbf{V} = V_c\nabla\phi,$$

where $\mathbf{V}$ is the vector velocity, ∇ is in units of tank radius for cylindrical coordinates, and V_c is a characteristic velocity defined such that the dimensionless velocity is a combination of Froude and Weber number,

$$\frac{V}{V_c} = \left[\frac{1}{\dfrac{gR}{\mathbf{V}^2} + \dfrac{\sigma}{\rho R\mathbf{V}^2}}\right]^{1/2} = \left[\frac{1}{\mathrm{Fr}} + \frac{1}{\mathrm{We}}\right]^{-1/2}. \tag{2}$$

At any solid wall, the normal velocity must be zero; hence,

$$\partial\phi/\partial\mathbf{n} = 0, \tag{3}$$

where $\mathbf{n}$ is a unit vector normal to the solid wall.

There are two conditions to be specified on the free surface. One condition defines the location of the free surface while the other condition gives the value of ϕ on the free surface. The two equations which result are coupled and must be solved simultaneously to fix the surface boundary condition on ϕ. The first relationship is termed the free-surface kinematic condition. It simply states that no fluid crosses the free surface. The free surface height is given by

$$\partial\xi/\partial t = (\partial\phi/\partial z) - \nabla\phi\cdot\nabla\xi. \tag{4}$$

The Bernoulli equation must hold throughout the fluid for inviscid flow. For irrotational flow, the constant in the Bernoulli equation is independent of streamline and may therefore be absorbed into the definition of ϕ. On the free surface, the Bernoulli equation is

$$\frac{\partial\phi}{\partial t} = -\frac{1}{2}\nabla\phi\cdot\nabla\phi - \frac{1}{1+\dfrac{1}{\mathrm{Bo}}}(\alpha_1(t)\,r\cos\theta + \alpha_2(t)\,r\sin\theta + (1+\alpha_3(t))\,\xi) + \frac{1}{1+\mathrm{Bo}}\nabla\cdot\left[\frac{\nabla\xi}{(1+\nabla\xi\cdot\nabla\xi)^{1/2}}\right], \tag{5}$$

where the accelerations, α_1, α_2 and α_3 are in units of the mean axial acceleration. α_3 must be periodic and small compared to 1, otherwise it is necessary to make the axial Bond number a function of time.

For the present problem, Eqs. (4) and (5) will be specialized to cylindrically symmetric flow. The free surface will be initially flat and in motion in a first mode slosh wave. The accelerations, α_1, α_2, and α_3 will be taken to be zero.

Application of the Galerkin Method

The method for solving the general boundary value problems first proposed by Galerkin [15] has been used extensively in solid mechanics problems. The Galerkin method has two distinct forms. The most widely known form applies to cases when solutions to the differential equation are not known, and the boundary conditions are homogeneous or are transformed to be homogeneous. A solution is postulated as a finite sequence of terms, each of which meet the boundary conditions. The coefficients of the sequence are found by taking the inner product of the differential equation with an appropriate set of weighting functions and solving the resultant matrix equation.

The less frequently encountered form of the Galerkin method is employed for the present problem. Particular solutions to the differential Eq. (1) are easily found. A sequence of these solutions that meets the solid-wall boundary conditions is found by separation of variables and set equal to the velocity potential

$$\phi = \sum_{n=1}^{N} A_n(t)[\cosh(\lambda_n z)/\cosh(\lambda_n h)]\, J_0(\lambda_n r), \tag{6}$$

where the A_n are coefficients to be determined from the the free-surface boundary conditions, h is the mean height of the free surface, and the λ_n are eigenvalues of the equations for the side-wall boundary condition,

$$(d/dr)[J_0(\lambda_n r)]_{r=1} = 0. \tag{7}$$

The free-surface boundary conditions (4) and (5) are parabolic and, therefore, can be integrated in time at a discrete set of points in space, given a sufficient set of initial conditions. Integration of the free-surface boundary equations through one time step leads to a new distribution of ϕ over a new free surface ξ. The new values of ϕ are equated to the sequence (6), evaluated at the new free surface,

$$\psi = \sum_{n=1}^{N} A_n \frac{\cosh[(\lambda_n(\xi + h))]}{\cosh(\lambda_n h)} J_0(\lambda_n r), \tag{8}$$

where ψ is used to represent the new numerical solution to (5) of the velocity potential on the free surface, matched by the expansion of ϕ (6).

The inner product of (8) with the weighting function, $rJ_0(\lambda_q r)$, is formed by numerical integration over the free surface (we used Simpson's rule and 51 points equally spaced on the radius). There results a matrix equation,

$$E_n \delta_{nq} = A_n I_{nq}, \tag{9}$$

where

$$E_n = K \int_0^1 \psi r J_0(\lambda_n r)\, dr,$$

$$I_{nq} = K \int_0^1 \left\{ \frac{\cosh[\lambda_n(\xi + h)]}{\cosh(\lambda_n h)} r J_0(\lambda_n r)\, J_0(\lambda_q r) \right\} dr$$

$$K = 2/J_0(\lambda_n),$$

and δ_{nq} is the Kronecker delta.

Equation (9) is solved by matrix inversion for the new A_n's in the sequence (6). Continuous updating of the A_n's is, of course, necessary so that current values of the spatial derivatives of ϕ may be calculated. The spatial derivatives of the surface shape are to be calculated from the expansion of the surface shape

$$\xi = \sum_{n=1}^{N} C_n J_0(\lambda_n r). \tag{10}$$

Repeated application of these computational steps in sequence gives a construction of the motion of the free surface as an initial value problem.

Calculation of Total System Energy

The figure of merit for this study is the total energy of the system. The total energy is comprised of kinetic, gravitational potential, and free-surface potential energies. The kinetic energy is given by

$$E_k = \iiint_V \tfrac{1}{2}\rho \nabla\Phi \cdot \nabla\Phi\, dV, \tag{11}$$

where ρ is the fluid density, and V is the volume. Equation (11) can be transformed by

$$\nabla\Phi \cdot \nabla\Phi = \nabla \cdot (\Phi \nabla\Phi) - \Phi \nabla^2\Phi. \tag{12}$$

The last term of (12) is zero by continuity. Equation (11) becomes

$$E_k = \frac{\rho}{2}\iiint_V \nabla \cdot (\Phi \nabla \Phi)\, dV = \frac{\rho}{2}\iint_S \Phi \nabla \Phi \cdot \mathbf{n}\, dS \tag{13}$$

by application of the divergence theorem. $\mathbf{n}$ is a unit outward directed normal to the free surface and the integral over the solid walls is zero by the boundary condition (3).

The elemental surface area is shown in Fig. 1 to be

$$ds = \sqrt{1 + f^2}\, r\, dr\, d\theta, \tag{14}$$

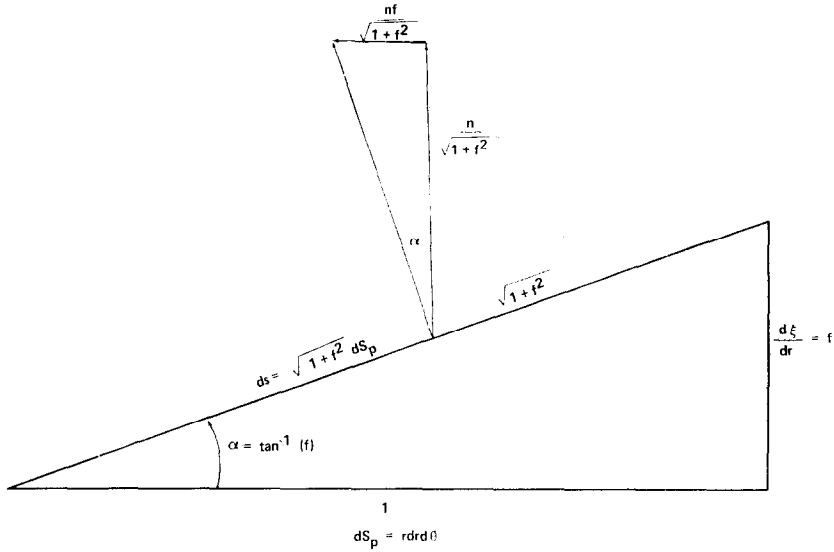

FIG. 1. Vector diagram of surface area and resolution of $\nabla\phi \cdot \mathbf{n}$.

where $f = d\xi/dr$, and $\nabla\Phi \cdot \mathbf{n}$ becomes

$$\nabla\Phi \cdot \mathbf{n} = \left(\frac{\partial \Phi}{\partial Z} - f\frac{\partial \Phi}{\partial R}\right)\Big/\sqrt{1 + f^2}, \tag{15}$$

giving the kinetic energy as

$$E_k = \frac{\rho}{2}\iint_S \Phi\left(\frac{\partial \Phi}{\partial Z} - f\frac{\partial \Phi}{\partial R}\right) r\, dr\, d\theta. \tag{16}$$

For a symmetric oscillation, it is sufficient to integrate in the peripheral direction through one radian. Equation (16) then reduces to

$$E_k = \frac{\rho}{2} \int_0^R \Phi \left(\frac{\partial \Phi}{\partial Z} - f \frac{\partial \Phi}{\partial R} \right) r \, dr.$$

In the combined Weber–Froude number system of nondimensionalization, the characteristic energy is

$$E_c = \rho g R^4 [1 + 1/\mathrm{Bo}]. \tag{17}$$

Dividing by E_c gives the dimensionless kinetic energy

$$e_k = \frac{1}{2} \int_0^1 \phi \left(\frac{\partial \phi}{\partial z} - f \frac{\partial \phi}{\partial r} \right) r \, dr. \tag{18}$$

The dimensionless gravitational potential energy is given by

$$\begin{aligned} e_g &= \frac{\mathrm{Bo}}{1 + \mathrm{Bo}} \int_0^\xi \int_0^1 \int_0^1 (z - z_0) \, r \, dr \, d\theta \, dz \\ &= \frac{1}{2} \frac{\mathrm{Bo}}{(1 + \mathrm{Bo})} \left[\int_0^1 (\xi + h - z_0)^2 \, r \, dr + \frac{z_0^2}{2} \right]. \end{aligned} \tag{19}$$

The reference height (z_0) is chosen to be the mean surface height (h) and the constant portion is dropped. The gravitational energy departure from the rest state is

$$e_g = \frac{1}{2} \left(\frac{\mathrm{Bo}}{1 + \mathrm{Bo}} \right) \int_0^1 \xi^2 \, r \, dr. \tag{20}$$

From the definition of the coefficient of surface tension, the increase of dimensionless free-surface energy from the rest state is

$$e_s = \frac{1}{1 + \mathrm{Bo}} \iint_s [ds - ds_p] = \frac{1}{1 + \mathrm{Bo}} \int_0^1 [\sqrt{1 + f^2} - 1] \, r \, dr. \tag{21}$$

The total energy is the sum of the three contributing energies,

$$\begin{aligned} e_t = \int_0^1 \Big[&\frac{\phi}{2} \left(\frac{\partial \phi}{\partial z} - f \frac{\partial \phi}{\partial r} \right) + \left(\frac{\mathrm{Bo}}{1 + \mathrm{Bo}} \right) \frac{\xi^2}{2} \\ &+ \left(\frac{1}{1 + \mathrm{Bo}} \right) (\sqrt{1 + f^2} - 1) \Big] \, r \, dr. \end{aligned} \tag{22}$$

3. General Description of Integration Techniques

Schemes for the solution of initial value problems are broadly classified as explicit, iterative, and implicit. These terms are easily defined by an example using the equation,

$$\partial f/\partial t = F(f, t). \tag{23}$$

Explicit methods predict the value of f at the end of a time step from information known at the beginning, as in the Euler method, a one-term Taylor expansion in time,

$$f^{n+1} = f^n + \delta t\, F^n, \tag{24}$$

where the superscripts refer to the time step or time level.

The explicit scheme of (24) is always unstable unless there is dissipation in the equations, as shown by Daly [7] and Hirt [8]. Hence, this scheme is not suitable for the present, nondissipative problem. There are also explicit schemes which are second order in time; that is, second-order Taylor expansions are approximated. These schemes may be well suited to the present problem. If (24) were written as

$$f^{n+1} = f^n + \delta t\, F^{n+1}, \tag{25}$$

the method would be called Euler-implicit because the right side depends on information which is not known until the left side is known. Successful solution depends on being able to substitute (25) into (23) and solve for either f^{n+1} or F^{n+1}. When there is a system of simultaneous equations to solve, as in the present problem where there may be 100 simultaneous equations for surface height and velocity potential at points on the surface, the resultant matrix manipulations become very difficult. The implicit scheme may be approximated by a two-step or iterative process,

$$\begin{aligned} f^* &= f^n + \delta t\, F^n \qquad \text{and} \\ f^{n+1} &= f^n + \delta t\, F^*. \end{aligned} \tag{26}$$

This method is variously known as Matsuno, Euler-backward, and, apparently incorrectly, as Euler-modified. In this scheme, f^* is presumed to be a good approximation to f^{n+1} if the time step is sufficiently short. Therefore, F^* is a good approximation to F^{n+1} and the method gives results which closely follow the implicit scheme of (23). Such schemes, known as iterative schemes, may also be well suited to the present problem.

Two explicit and four iterative methods were selected for further study. These methods are described in Table I and known features of the methods are reviewed. These schemes are all well known, and will not be described here. The reader who desires more information can find derivations in many references including Easton [13].

TABLE I

Explicit and Iterative Methods

Class	Method	Equations	Linearized stable time[a] $p = \lambda c\, \delta t$	Linearized amplification factor
Explicit	Adams–Bashforth	$f^{n+1} = f^n + \delta t(1.5F^n - 0.5F^{n-1})$	Slightly unstable	$\sqrt{1 + p^4/4}$
	Leapfrog (time centered, midpoint rule)	$f^{n+1} = f^{n-1} + 2\delta t F^n$	$p = 1$	1
Iterative	Matsuno (Euler backward)	$f^* = f^n + \delta t\, F^n$ $f^{n+1} = f^n + \delta t\, F^*$	$p = 1$	$\sqrt{1 - p^2 + p^4}$
	Heun (Euler trapezoidal)	$f^* = f^n + \delta t\, F^n$ $f^{n+1} = f^* + \delta t/2(F^* - F^n)$	Very slightly unstable	$\sqrt{1 + p^4/4}$
	Leapfrog trapezoidal	$f^* = f^{n-1} + 2\delta t\, F^n$ $f^{n+1} = f^n + \delta t/2(F^n + F^*)$	$p = \sqrt{2}$	$\sqrt{1 - (p/2)^4}$ [b]
	Lax–Wendroff	$f^* = f^n + \delta t/2F^n$ $f^{n+1} = f^n + \delta t F^*$	Slightly unstable	$\sqrt{1 + p^4/4}$ [c]

[a] Times are given by Kurihara for the wave equation $df/dt = -i\lambda cf$.

[b] Approximate relationship by Easton.

[c] Damping found by Lilly was an effect of the spatial differencing.

4. Effects of Nonlinearities on Truncation Errors

A simple case was set up to test the effects of the particular set of nonlinearities of this problem on the various integration methods. The problem chosen was that of a symmetric free oscillation with an initial condition of a flat surface and a velocity potential specified by

$$\phi = 0.05 J_0(\lambda_1 r), \tag{27}$$

where $\lambda_1 = 3.831706$ is the first symmetric eigenvalue.

This problem is particularly difficult for numerical integration because it represents an initial missmatching of the amplitudes of the harmonics to the fundamental mode. In a real free oscillation, it would not be expected that all harmonics have zero amplitude for both the surface shape and the surface velocity potential simultaneously. The problem is simplified in the sense there is no mechanism whereby energy can be transferred from the symmetric oscillation to asymmetric oscillations.

The six promising integration methods, Adams–Bashforth, leapfrog, leapfrog trapezoidal, Heun, Euler-backward, and Lax–Wendroff, were used.

A history of the total energy in a symmetric free oscillation is shown in Fig. 2 for the six selected integration methods with a step of 0.025. Note that all six of the methods show an oscillation in the total energy. The oscillation appears to be unavoidable for these integration schemes when applied to a nonlinear advection problem. The source of the osicillation is not apparent, but seems to be related to the nonlinear interaction between oscillation modes. The more important question is whether there are long-term trends to these oscillations. That is, does the mean energy grow or decay? In the upper curve the calculations, using the Adams–Bashforth method, clearly show an increase in the mean value of total energy. In fact, this method is numerically unstable for this free-oscillation problem. A smaller initial amplitude would give a much more stable behavior for the Adams–Bashforth method. The increase of total energy was also reported by Lilly [12]. The leapfrog and Lax–Wendroff methods were indistinguishable on the scale of this plot. The existence of a long-term trend is not apparent in this plot, but the leapfrog method did show a catastrophic increase of energy at longer time, as shown in Fig. 3. The total energy follows the same pattern found by Lilly of increasing oscillation amplitude, together with an increasing mean total energy, leading to an eventual instability.

The leapfrog trapezoidal and Heun methods are seen in Fig. 2 to follow the same general trend as the leapfrog method with the difference that rate of growth of total energy is slower. The Euler-backward method, as previously mentioned, shows rather strong damping, but it is the only method of those tested which does show damping at a time step of 0.025.

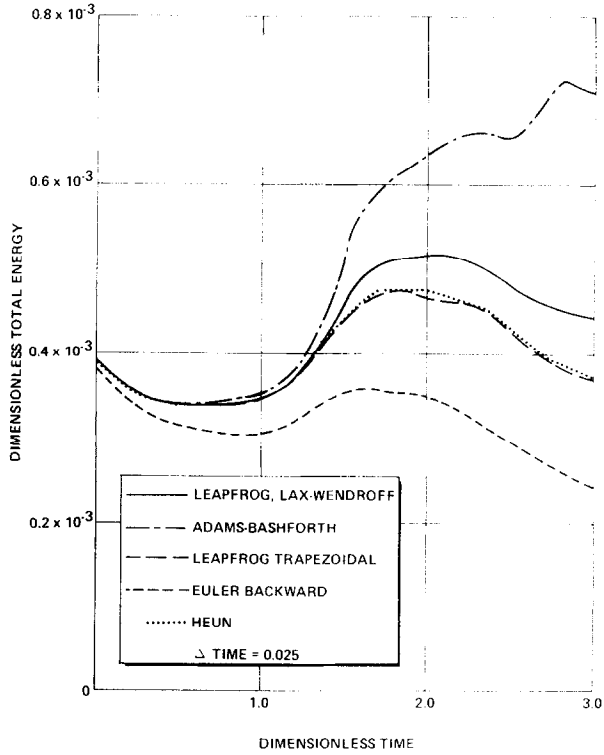

FIG. 2. Total energy history for a symmetric, free oscillation.

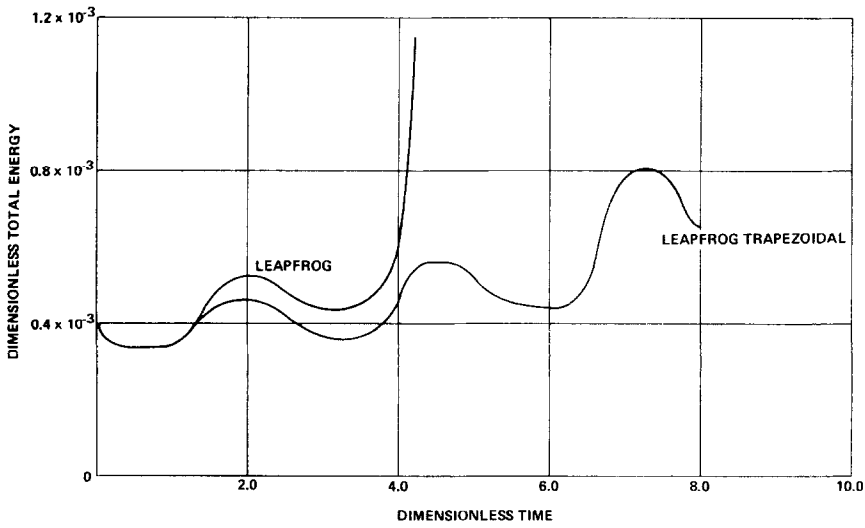

FIG. 3. Total energy history for leapfrog and leapfrog trapezoidal methods.

A check of numerical consistency was run by plotting the total energy at a specified time against the length of time step (Fig. 4). A numerically-consistent scheme should converge toward the initial energy as the time step becomes very short. However, the oscillation of the total energy would prevent these methods from converging to the initial total energy. The leapfrog trapezoidal and Heun

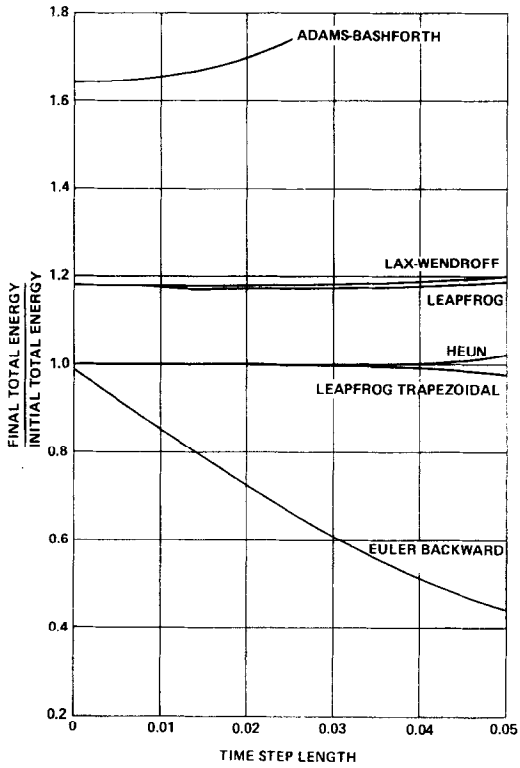

FIG. 4. Total energy dependence on time step length at dimensionless time = 3.0.

methods appear to be the most accurate, hence they will be taken as the norm. In Fig. 4, the value of total energy at time = 3.0 is ratioed to the value for the leapfrog trapezoidal method with a short time step. Time steps of 0.0125, 0.025, 0.0375, and 0.05 were chosen. The time when the comparisons were made (3.0) corresponds to the maximum time in Fig. 2.

The results of Fig. 4 compare quite well with those published by Kurihara [11]. All second-order techniques approach a horizontal tangency as the time step is reduced toward zero. The Adams–Bashforth method is seen to produce an increase of total energy that depends only mildly on the length of the time step, but this

method diverges for the larger time steps. Hence, care must be taken to keep the time step small when using this method. It can be assumed with confidence that the solution using Adams–Bashforth is bounded if the time step and total time are sufficiently short. The leapfrog and Lax–Wendroff methods have a lesser dependence on time step, but both methods do seem to amplify the total energy.

The Euler-backward method shows damping that increases strongly with the length of the time step. Whether the method is numerically consistent could not be determined from the four time steps used. By adding a fifth step, at $\delta t = 0.005$, the method is shown to be numerically consistent. Figure 5 shows that the history of total energy for the Euler-backward method approaches that of the leapfrog trapezoidal method for a sufficiently short time step.

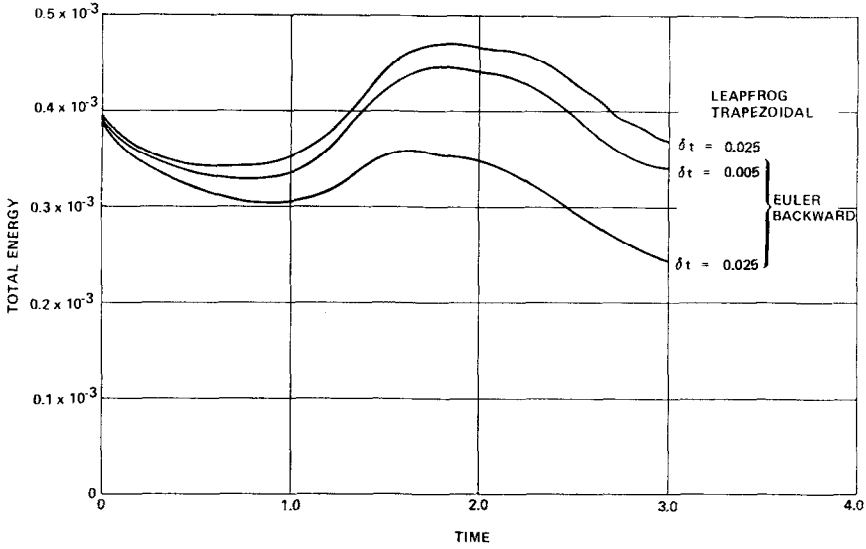

FIG. 5. Total energy history dependence on length of time step.

The total energy is a very sensitive measure of the accuracy of a solution technique. Figure 6 shows a comparison of the surface shape for six integration methods at a time = 2.0 near an extreme of the surface. On the left side, the leapfrog trapezoidal technique is compared to the Adams–Bashforth technique. Despite the fact that the Adams–Bashforth curve contains 70 % more energy than the leapfrog trapezoidal, there is only a small difference in the surface shape that shows up as a difference in higher harmonics. The leapfrog and Lax–Wendroff methods show virtually the same result as the leapfrog trapezoidal and Heun, and the Euler-backward method approaches these very closely for a small time step.

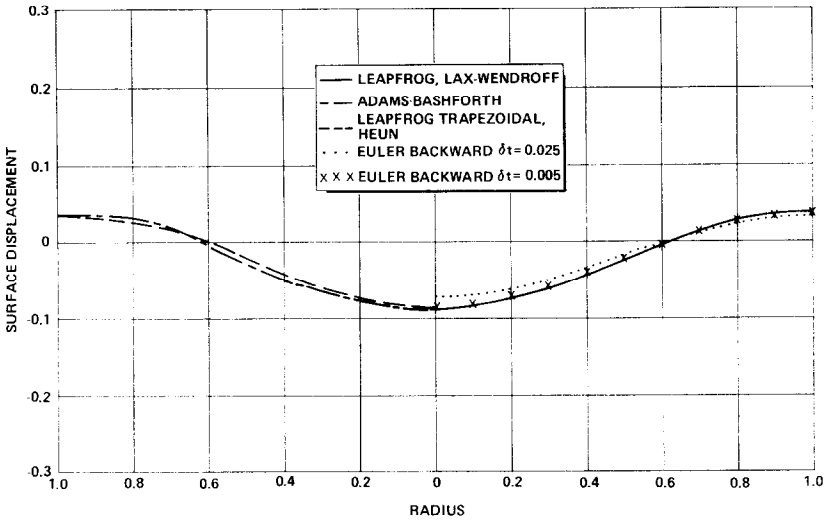

FIG. 6. Dependence of free-surface shape on integration method.

5. CONCLUSIONS

It might be expected then that the leapfrog trapezoidal or Heun method would be the optimum method for solving the potential flow problem. Indeed, they probably would be the optimum methods for solving a dissipative problem. But for the present nondissipative problem, two irreconcilable difficulties arise. First, the time step required to introduce any damping into the primary wave to control an insipient numerical instability shown by Easton [13] is quite large for the leapfrog trapezoidal method. Damping cannot be induced by the Heun method. Second, a time step sufficiently large to introduce damping is too large if many modes and harmonics of oscillation are desired in the solution, and the solution again becomes unstable. The problem becomes compounded when the higher modes tend to be captured by the nonlinear interaction of the lower modes and to not behave as free oscillations. This point is illustrated in Fig. 7, where the coefficients of the sixth harmonic of the first symmetric mode are plotted against time for a free oscillation. The wave height and velocity potential begin 90° out of phase, as in a free oscillation, but are soon changed and bear no resemblance to the free oscillations as time goes on. This phenomenon, called entrainment of frequency, is characteristic of nonlinear oscillations and was reported to have been observed experimentally by Ladeke [16]. The result of entrainment of frequency is that the actual period of the higher harmonics may be much less than the natural free-oscillation period.

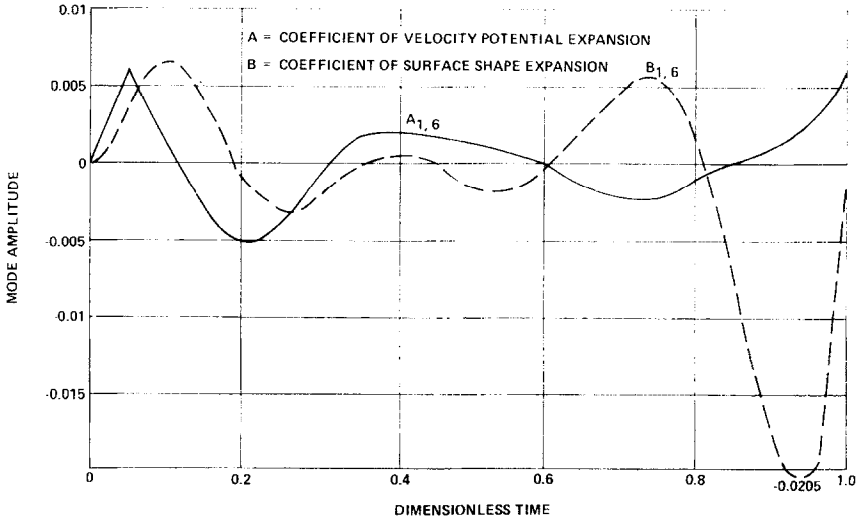

FIG. 7. Amplitude history of velocity potential and surface displacement.

The conclusion from the above study is that for short times, any of the integration methods above would be acceptable; for longer times, the Euler-backward method is the only method that has sufficient damping to control the incipient instability of the equations. The method to be used should be selected in accordance with the need of the particular problem in question.

ACKNOWLEDGMENT

The research described here was conducted by the McDonnell Douglas Astronautics Company-West as part of the Independent Research and Development Program.

REFERENCES

1. F. H. HARLOW AND J. E. WELCH, Numerical calculation of time dependent viscous incompressible flow, *Phys. Fluids* **8** (1965), 2182.
2. C. R. EASTON AND I. CATTON, Nonlinear free surface effects in tank draining at low gravity, AIAA *Journal* **8** (1970), 2195.
3. R. E. MOORE AND L. M. PERKO, Inviscid fluid flow in an accelerating cylindrical container, *J. Fluid Mech.* **22** (1965), 305.
4. R. E. HUTTON, "An Investigation of Resonant Nonlinear, Nonplanar Free-surface Oscillations of a Fluid," Ph.D. Thesis, Univ. Calif., Los Angeles, CA, 1963.
5. J. W. THOMAS, "On the Exact Form of Gravity Waves on the Surface of an Inviscid Liquid," Ph.D. Thesis, Arizona University, Tucson, AZ, (1967).

6. D. CRAPPER, An exact solution for progressive capillary waves of arbitrary amplitude, *J. Fluid Mech.* **2** (1957), 532.
7. B. J. DALY, The stability properties of a coupled pair of nonlinear partial difference equations, *Math. Comp.* **17** (1963), 346–360.
8. C. W. HIRT, Heuristic stability theory for finite difference equations, *J. Computational Phys.* **2** (1968), 339.
9. L. M. PERKO, Large-amplitude motions of a liquid–vapour interface in an accelerating container, *J. Fluid Mech.* **35** (1969), 77.
10. M. P. HOLLISTER, H. M. SATTERLEE, AND H. COHAN, "A Study of Liquid Propellant Behavior During Periods of Varying Accelerations," LSML-A874728, Lockheed Missiles and Space Company, Sunnyvale, CA, 1967.
11. Y. KURIHARA, On the use of implicit and iternative methods for the time integration of the wave equation, *Monthly Weather Rev.* **93** (1965), 33–45.
12. D. K. LILLY, On the computational stability of numerical solutions of time dependent nonlinear geophysical fluid dynamics problems, *Monthly Weather Rev.* **93** (1965), 11–26.
13. C. R. EASTON, Large amplitude free surface oscillations with surface tension, Ph.D. Thesis, School of Engineering and Applied Sciences, Univ. Calif., Los Angeles, CA, 1970.
14. SIR HORACE LAMB, "Hydrodynamics," 6th ed., Cambridge Univ. Press, London, 1932.
15. B. G. GALERKIN, Series solutions of some problems of elastic equilibrium of rods and plates, *Vestn. Inzhenelrov* (in Russian), **1** (1915), 879–901.
16. C. A. LUDEKE, Nonlinear phenomena, Trans. ASME, **79** (1957), 439.